AIChE InterScience DISCOVER SOMETHING GREAT

FLUID MECHANICS AND TRANSPORT PHENOMENA

Derivation, Simulation and Validation of a Cohesive Particle Flow CFD Model

Berend van Wachem and Srdjan Sasic
Dept. of Applied Mechanics, Chalmers University of Technology, Gothenburg, Sweden

DOI 10.1002/aic.11335
Published online November 5, 2007 in Wiley InterScience (www.interscience.wiley.com).

A comprehensive physical model describing the agglomeration behavior present during fluidization of fine powders is still missing in literature. A model of balance of forces acting on a single solid particle is introduced, aiming at predicting and locally estimating the size of the agglomerates created in the bed. Computational fluid dynamics (CFD) have been used to investigate the hydrodynamics of a gas-solid fluidized bed operated with particles belonging to group A of Geldart classification.[1] *The key issue is that, in the gas and particle flow field, both hydrodynamic and interparticle forces are of importance. The model is incorporated into simulations based on an Eulerian approach and using the kinetic theory of granular flow. In the simulations, the closure models describing the hydrodynamics of the solids phase are directly affected by the behavior of the agglomerates. No empirical data or parameters were used to close the model. The simulations are compared with experiments of an independent research group, through the time-averaged solids volume fraction in a fluidized bed operated at different gas velocities. The agreement obtained between the simulation results and data from the literature is very good. Also, it is shown that, under flow conditions treated in this work, agglomerates of size of several single particle diameters are present in the fluidized bed.* © 2007 American Institute of Chemical Engineers *AIChE J,* 54: 9–19, 2008

Keywords: cohesive particles, fluidization, numerical simulations, Geldart A particles, agglomeration

Introduction

The gas-solid fluidized bed has proved a very useful type of reactor for a large number of devices in industrial practice. Although fluidized beds are widely used in many types of industries, there are two main fields of application: chemical engineering and energy conversion. Fluid catalytic cracking (FCC), mixing of powders, to name a few, belong to the former group,[2] whereas steam and hot water production in boilers is the main application in the energy conversion field. The understanding of the processes taking place in both types of applications is impeded by the complexity of fluidized-bed processes. A comprehensive description requires information on fluid-mechanics, heat transfer, chemical reaction, thermodynamics, and, at the same time, on awareness of the coupling of these phenomena. However, it is generally accepted that fluid dynamics predominantly govern the processes involved, and, therefore, fluid dynamics need to be explained in the first place to understand the overall behavior of the system. For that purpose, computational fluid dynamics (CFD) have in the last two decades proved a useful tool, which offers a comprehensive approach to understanding the phenomena that occur between the phases in fluidized-bed reactors. The current work employs CFD to understand and predict the agglomeration process occurring in fluidized-bed reactors with fine particles.

A correct perception of the dominant forces acting on a solid particle in a fluidized-bed reactor is essential to accu-

Correspondence concerning this article should be addressed to B. van Wachem at berend@chalmers.com.

rately predict its behavior. One of the key parameters that affects the force balance is the type of solid particles used in the application of interest. Geldart[1] classified powders into four groups, and with respect to the investigations of the hydrodynamics in the form of numerical simulations, literature is undoubtedly dominated by the studies of the more coarse Geldart B and D particles. On the other hand, there is a relatively limited number of studies dealing with simulations of the fluid dynamics of reactors operated with fine particles, or Geldart A particles, although these are considered of high-relevance for industrial applications, predominantly in FCC units, as mentioned above. The present work, therefore, aims at resolving some of the difficulties in CFD model development for fine particles. These difficulties may be attributed to the fundamental feature of the flows involving group A particles: interparticle forces, most often negligible in flows when larger particles are involved, here play an important role. As a consequence of the latter, there is a tendency that agglomerates are formed in the bed, which, in turn, significantly affects the flow field. This process is not to be confused with clustering; although both of them result in reduction in the number and increase in the size of particles, in fluidization literature it is generally assumed that clustering occurs due to hydrodynamic forces, whereas with agglomeration, it is cohesive forces that give rise to the binding of particles.

Both Lagrangian and Eulerian models have been applied to model the solid phase in fluidized-bed reactors involving Geldart A particles, and with varying success. In brief, in the Lagrangian models individual particles are tracked as they move through the domain, and the reference frame moves with the particles. When applied to granular systems, such models are referred to as discrete element methods (DEM) or a particle-tracking approach. The gas-flow field is resolved at a larger scale than the size of the particles (a computational cell usually contains up to 10^2 particles), and the maximum total number of particles simulated is of the order of 10^6, or even higher,[3] depending on the conditions and employed models. The motion of particles is obtained directly by solving the Newtonian equation of motion with, possibly, involving a model to handle nonideal particle–particle interactions (e.g. collisions).

An alternative to tracking individual particles is to perform a statistical averaging of the governing equations describing the behavior of the particles, presenting both phases as interpenetrating continua (the so-called two-fluid models), and where interfacial terms, stress tensors and turbulence, if any, require closure modeling. The approach to model the subgrid behavior of the particles and dominant in literature at present, uses the kinetic theory of granular flow, derived in analogy with the kinetic theory of gases.[4] The concept of granular temperature is introduced as a measure of kinetic energy of the random motion of particles. A detailed explanation of the derivation procedure, including a discussion on differences in the resulting equations, and the consequences on the flow field predictions can be found in Enwald et al.[5] or Van Wachem et al.[6] Within the framework of the Lagrangian modeling, it is straightforward to include the cohesive nature of fine particles. It is, however, questionable if the true agglomeration effect seen in Lagrangian simulations is due to the too large length-scale of the gas-phase resolution. Moreover, the Lagrangian approach is limited to computations in relatively small domains, which makes it still unusable for simulations of processes of larger scale.

As for the Eulerian models, the inability of classic two-fluid approaches to accurately represent the fluid dynamics of FCC particles was first recognized by Ferschneider and Mege,[7] when a severe overestimation of the bed expansion was observed in the simulations. Krishna and van Baten[8] employed the two-phase theory of fluidization, and set the bubble and emulsion phase as the two fluids. The problem in this approach is to determine and employ the true bubble (dense phase) and emulsion properties, as well as to clarify the solids behavior and its interaction with the gas phase. Mc Keen and Pugsley[9] suggested that the agglomeration of particles results in larger effective particle sizes and, consequently, in reduced relative drag forces. To reduce the drag force, they proposed an empirical scale factor of the drag force. Unfortunately, such an empirical scale factor needs to be retuned for every type of particle, and for each fluidization condition. A recent study by the same research group[10] provided a more detailed theoretical explanation for the reduction of the drag force. In a similar attempt to modify the drag force, Zimmermann and Taghipour[11] empirically shifted the minimum fluidization velocity in the simulations to match experiments. Although this might give a satisfying prediction for the minimum fluidization velocity, it lacks both generality and physical background.

A different approach is taken by Kim and Arastoopour[12]: they modified the kinetic theory of granular flow aiming at including a complex cohesive force model. The approach resulted in derivation of the new governing equations and closure models (primarily for the stresses of the particulate phase) for the flow involving cohesive particles. However, the application of the model is limited due the necessity of introducing such inputs whose definition and evaluation may become unclear (such as the definition of the contact bonding energy between solid particles). Moreover, one of the most important issues, the effect of the drag force, is not discussed or taken into account.

In a similar approach to modify the closure models for the presence of cohesive forces, Gidaspow and Hullin[13] have incorporated the empirically determined cohesive pressure into the term representing the particle pressure. As a consequence, the particle pressure predicted by the proposed model became larger than the pressure obtained by the kinetic theory of granular flow for flows of noncohesive particles. Finally, Ye et al.[14] have modified the kinetic theory approach by adding an excess compressibility term that accounts for the effect of cohesion between particles. These models may provide valuable information in relation to general aspects of modeling flows of mixtures involving cohesive particles. However, these models contain a number of empirical constants, of which the magnitude is not always clear.

Although the cohesive force can be readily modeled in the Lagrangian framework, it was indicated earlier that this is quite difficult in the Eulerian approach. In this work, we aim at locally estimating the size of agglomerates in the Eulerian framework, by modeling the cohesive mechanism. With the local size of the agglomerates, the closure models describing the hydrodynamics of the solids phase can be adjusted. Therefore, we have chosen here not to directly

modify the particle pressure term; it is the employment of the agglomerate diameter in the kinetic theory framework that will lead to an increased production of granular temperature and, consequently, of granular pressure. The size of the agglomerates is determined by a force balance including, next to the common hydrodynamic forces, the cohesive interparticle forces.

Theory

The goal of the current work is to derive a model that predicts the size of the agglomerates formed in a gas-solid flow with fine particles, and to combine this model with CFD calculations of realistic operating conditions of a fluidized bed. The size of the agglomerates is calculated by considering all forces locally acting on the solid particles. Considering a mixture of gas and fine particles, such as in a fluidized bed with Geldart A particles, a number of important forces can be recognized. These are the hydrodynamic (or drag) forces, the gravity and buoyancy forces, the particle–particle collisional forces, and the interparticle cohesive forces. These forces will be discussed individually prior to deriving the agglomerate model.

Hydrodynamic forces

Generally, when modeling the momentum transfer between the gas and the particles, the form and skin drag on the particles are combined in one force, the interphase drag force. In the studies related to fluidization, the drag force is typically obtained from pressure drop measurements in fixed, fluidized or settling beds. Although there is a large number of drag force models described in the literature, we have adopted here the one proposed by Wen and Yu.[15] The model chosen was shown to be applicable for studies of fluid dynamics of fluidized beds, see van Wachem and coworkers.[6] This drag force expression incorporates experimental data over the whole range of solids volume fractions. The drag force is given by

$$\boldsymbol{F}_{\text{drag}} = \frac{3}{4} C_d \frac{(1-\epsilon)\epsilon\rho_f |(\boldsymbol{u}_f - \boldsymbol{u}_p)| (\boldsymbol{u}_f - \boldsymbol{u}_p)}{d_p} (1-\epsilon)^{-2.65} \quad (1)$$

where ρ_f is the fluid density, $\boldsymbol{u}_f$ and $\boldsymbol{u}_p$ are the gas and particles velocities. ε is the volume fraction of the particulate phase, and d_p represents the mean diameter of the particles. The drag coefficient C_d is given by

$$C_d = \begin{cases} \dfrac{24\left(1 + 015((1-\epsilon)R_e)^{0.687}\right)}{R_e(1-\epsilon)}(1-\epsilon)^{-2.65} & \text{if } (1-\epsilon)R_e < 1000 \\ 0.44 & \text{if } (1-\epsilon)R_e \geq 1000 \end{cases} \quad (2)$$

and the particle Reynolds number is defined as

$$R_e = \frac{d_p \rho_g |\boldsymbol{u}_p - \boldsymbol{u}_f|}{\mu_g} \quad (3)$$

This form of the drag force model will represent the hydrodynamic forces on the particles. It is noted by Wen and Yu[15] that this model is valid to predict the drag force on fine particles as well. The choice of the drag model and its consequences to the model proposed in this work will be further discussed in the following.

Gravity force

The gravity and buoyancy forces are given by

$$F_{\text{grav}} = \frac{\pi}{6}(\rho_p - \rho_f) d_p^3 g \quad (4)$$

Collisional forces

When the volume fraction increases over a tenth of a percent, particle-particle interactions become an important physical mechanism. There are various ways to deal with such interactions. Walton[16] showed that the theory of elasticity[17] is a valid approach to model individual particle-particle interactions. According to the theory of elasticity, if solid particles are assumed nearly elastic and that they collide with a relative velocity V, the displacement of the maximum compression is given by

$$\alpha = \left(\frac{5}{4}\frac{V^2}{n n_1}\right)^{2/5} \quad (5)$$

where n and n_1 are given by

$$n = \sqrt{\frac{8}{9\pi^2(k_1 + k_2)}\frac{d_{p_1} d_{p_2}}{d_{p_1} + d_{p_2}}} \quad (6)$$

$$n_1 = \frac{m_1 + m_2}{m_1 m_2} \quad (7)$$

and m_1 and m_2 denote the masses of the two colliding particles, and d_{p_1} and d_{p_2} their diameters. When the particles are of the same type

$$k_1 = k_2 = k = \frac{1 - v^2}{\pi E} \quad (8)$$

where v is the Poisson's ratio, and E the Young's modulus of the particles. The equation for the maximum compression then becomes

$$\alpha = \left(\frac{5V^2\pi^2 k \rho_p d_{p_1}^3 d_{p_2}^3}{8\left(d_{p_1}^3 + d_{p_2}^3\right)}\sqrt{\frac{d_{p_1} + d_{p_2}}{d_{p_1} d_{p_2}}}\right)^{2/5} \quad (9)$$

and the resulting colliding force

$$F_c = n\alpha^{3/2} = 0.2516\left(\frac{V^6\pi\rho_p^3}{k^2}\left(\frac{d_{p_1}^3 d_{p_2}^3}{d_{p_1}^3 + d_{p_2}^3}\right)^3 \frac{2d_{p_1}d_{p_2}}{d_{p_1}+d_{p_2}}\right)^{1/5} \tag{10}$$

with $d_{p1} = \Phi d_{p2}$

$$F_c = 0.166\left(\frac{\pi V^6\rho_p^3}{k^2}\right)^{1/5}\left(\frac{2^4\Phi^{10}}{\left(1+\Phi^3\right)^3(1+\Phi)}\right)^{1/5} d_{p_1}^2 \tag{11}$$

This force represents the force on a particle due to particle collisions in the flow.

Cohesive forces

The major difference in the hydrodynamic behavior of fine particles and large particles originates from the presence of cohesive forces. Although such forces can be of significance in the flow behavior of larger particles as well, their relative meaning is most often negligible. In the flow behavior of fine particles, however, the relative meaning of cohesive forces is often dominant.

Since particles in the present work are assumed dry (i.e. there are no liquid bonds that would additionally contribute to the creation of the agglomerates), the mechanism behind the cohesiveness of such particles is generally believed to be the Van der Waals force.[18] The van der Waals force between two spherical particles can be expressed as

$$F_{va} = \frac{A}{12\delta^2}\frac{d_{p_1}d_{p_2}}{d_{p_1}+d_{p_2}} \tag{12}$$

where A is the Hamaker constant, which is related to the type of material, and δ is the distance between the particles. If the particles have the same size, this equation further simplifies to

$$F_{va} = \frac{Ad_p}{24\delta^2} \tag{13}$$

One of the key parameters of the model is the Hamaker constant, which will be discussed later.

Balance of forces

The agglomerate model proposed and utilized here is an extension of the model developed by Zhou and Li,[19] with significant differences in the resulting expression for the agglomerate diameter. The four most important forces, acting on a particle when fine powders are fluidized, are used to formulate a local force balance. If the forces acting on a single particle are considered, a simple balance can be derived

$$F_{grav} + F_{va} = F_{drag} + F_c \tag{14}$$

The key assumption here is that there is a clear separation of time scales between agglomeration of particles and their mean advection through the bed; the model assumes that particles agglomerate considerably faster compared to their mean vertical movement in the bed. The latter statement can be supported by the fact that, under conditions used for simulations in this work, the cohesive force can be up to a order of magnitude larger than the gravity and hydrodynamic forces, responsible for the large-scale movement in the bed. In addition, and equally supportive for the validity of the approach proposed here, the separation of time scales has been previously observed in DEM simulations of fluidized beds.[20] Hence, transient effects can be safely omitted, as a first approximation of course. However, the necessity of introducing such an approximation once again clearly illustrates the difficulties encountered in the Eulerian-Eulerian modeling of flows involving FCC particles.

When employing the expressions for the forces presented in the previous sections, the balance becomes a fourth order polynomial in the particle diameter. However, this equation will typically not be satisfied for the particle diameter d_p, as the particles can locally form agglomerates. Therefore, Eq. 14 is employed to determine the size of the local agglomerates, d_a, taking the size d_p as a starting point. For the agglomerate size on the other hand, d_a, it is assumed that the force balance Eq. (14) is fulfilled. The balance equation also accounts for the difference between the particle density and the agglomerate density. Thus

$$a_1 d_a^4 + a_2 d_a^3 + a_3 d_a^2 + a_4 = 0 \tag{15}$$

with

$$a_1 = \frac{\pi}{6}(\rho_a - \rho_g)g \tag{16}$$

$$a_2 = -0.166\left(\frac{\pi V^6\rho_a^3}{k^2}\right)^{1/5}\left(\frac{2^4\Phi^{10}}{\left(1+\Phi^3\right)^3(1+\Phi)}\right)^{1/5} \tag{17}$$

$$a_3 = \frac{A}{12\delta^2}\frac{1}{1+\Phi} \tag{18}$$

and

$$a_4 = -\frac{3}{4}C_d(1-\epsilon)\epsilon\rho_f\left(u_f - u_p\right)^2(1-\epsilon)^{-2.65} \tag{19}$$

and d_a is the characteristic size of the local agglomerates. Note that the parameter a_4 in Eq. 15 only seemingly comes in as a constant. In general, that term depends on the particle Reynolds number, which is a function of the size of the agglomerate. The fact that the term a_4 is also an explicit function of d_a is taken into account during the calculation procedure. The polynomial obtained is of the fourth order, and its solution is far from trivial. The details on the solution procedure and the meaning of the solutions will be discussed later.

Governing equations

The CFD model used in this work is based on the Eulerian-Eulerian model, where the gas and solid phases are both considered continuous and fully interpenetrating. Here, the general equations for the phases treated will be given; the changes due to the inclusion of the agglomerate model will be seen in terms needed to close the two-fluid model. The continuity equation for phase i (f-fluid, s-solid) is given by

$$\frac{\partial}{\partial t}(\epsilon_i \rho_i) + \nabla \cdot (\epsilon_i \rho_i \mathbf{v}_i) = 0 \tag{20}$$

where ε is the volume fraction of each phase, so $\epsilon_f + \epsilon_s = 1$. $\mathbf{v}$ represents the velocity, and ρ the density. The momentum equations for the gas phase is given by

$$\frac{\partial}{\partial t}(\epsilon_f \rho_f \mathbf{v}_f) + \nabla \cdot (\epsilon_f \rho_f \mathbf{v}_f \mathbf{v}_f) = \nabla \cdot \bar{\bar{\tau}}_f + \epsilon_f \rho_f \mathbf{g} - \epsilon_f \nabla P - \beta(\mathbf{v}_f - \mathbf{v}_s) \tag{21}$$

where $\bar{\bar{\tau}}$ is the viscous stress tensor, $\mathbf{g}$ is the gravity acceleration, P is the thermodynamic pressure, and β is the interphase momentum-transfer coefficient, which is directly related to the drag force discussed earlier. The solids phase momentum balance is given by

$$\frac{\partial}{\partial t}(\epsilon_s \rho_s \mathbf{v}_s) + \nabla \cdot (\epsilon_s \rho_s \mathbf{v}_s \mathbf{v}_s) = \nabla \cdot \bar{\bar{\tau}}_s + \epsilon_s \rho_s \mathbf{g} - \epsilon_s \nabla P - \nabla P_s^* + \beta(\mathbf{v}_f - \mathbf{v}_s) \tag{22}$$

where P_s^* is the solids pressure, and τ_s is the solids stress terms, which are both closed with the kinetic theory for granular flow.

Kinetic theory of granular flow Equivalent to the thermodynamic temperature for gases, the granular temperature can be introduced, as a measure for the energy of the fluctuating velocity of the particles. The granular temperature is defined as

$$\Theta_s = \frac{1}{3}\mathbf{v}_\mathbf{s}'^2 \tag{23}$$

where Θ_s is the granular temperature, and $\mathbf{v}_s'$ is the solids fluctuating velocity. The equation of conservation of the solids fluctuating energy can be found in Ding and Gidaspow[21]

$$\frac{3}{2}\left[\frac{\partial}{\partial t}(\epsilon_s \rho_s \Theta_s) + \nabla \cdot (\epsilon_s \rho_s \Theta_s)\mathbf{v}_\mathbf{s}\right] = \left(-\nabla P_s^* \bar{\bar{I}} + \bar{\bar{\tau}}_s\right) : \nabla \mathbf{v}_\mathbf{s} + \nabla \cdot (k_\Theta \nabla \Theta_s) - \gamma_\Theta + \Phi_\Theta \tag{24}$$

where k_Θ is the diffusion coefficient, γ_Θ is the dissipation of fluctuating energy, and Φ_Θ is the exchange of fluctuating energy between the phases.

The following expressions describe the hydrodynamics of the solid phase. Note that the expressions are adjusted for the presence of agglomerates (index a is used instead of s).

The dissipation of fluctuating energy is described by Jenkins and Savage[22]

$$\gamma_\Theta = 3(1 - e^2)\epsilon_a^2 \rho_a g_0 \Theta_a \left(\frac{4}{d_a}\sqrt{\frac{\Theta_a}{\pi}} - \nabla \cdot \mathbf{v}_a\right) \tag{25}$$

where g_0 is the radial distribution function, which is discussed below, e is the coefficient of restitution of colliding particles, and d_a is the size of the local agglomerates.

In this work, the algebraic model is used to calculate the granular temperature. The models assumes that the granular energy is dissipated locally, and only generation and dissipation terms are to be retained. The procedure has been proven correct for simulations of noncirculating beds.[6] Additional tests have been made including the full transport equation, with suppressing only the exchange of fluctuating energy between the phases. The latter is carried out having in mind that the gas-phase turbulence is particularly suppressed in noncirculating fluidized beds. No significant differences were observed between the two cases.

The solids pressure represents the solids phase normal forces due to particle–particle interactions. Its description based on the kinetic theory of granular flow was developed by Jenkins and Savage[22] and Lun et al.[4] In this approach both the kinetic and the collisional influences are taken into account. The kinetic part describes the influence of particle translations, whereas the collisional term accounts for the momentum transfer by direct collisions. The solids pressure of Lun et al.[4] is used in this work

$$P_a^* = \epsilon_a \rho_a \Theta_a (1 + 2 g_0 \epsilon_a (1 + e)) \tag{26}$$

The bulk viscosity is a measure for the resistance of a fluid against compression. It is obvious that the importance of the bulk viscosity depends strongly on the velocity gradients. In a fluidized bed, the bulk viscosity and the shear viscosity are in the same order of magnitude, and, thus, the bulk viscosity should not be neglected, as is done in simulating Newtonian fluids. The equation of Lun et al.[14] is used in this work

$$\lambda_a = \frac{4}{3}\epsilon_a \rho_a d_a g_0 (1 + e)\sqrt{\frac{\Theta_a}{\pi}} \tag{27}$$

where λ_a is the bulk viscosity of the solids phase.

While the pressure and the bulk viscosity describe the normal forces, the shear viscosity accounts for the tangential forces. It was shown by Lun et al.[4] that it is possible to combine different interparticle forces and to use a momentum balance similar to that of a true continuous fluid. Similar to the solids pressure, the solids phase viscosity can be derived from the kinetic theory. The shear viscosity is builtup out of two terms : one term for the dilute region and one term for the dense region. In literature different expressions for the solids shear viscosity can be found. In this work the approach of Gidaspow et al.[23] is used, because this approach is validated by comparison with measured data

$$\mu_a = \frac{4}{5}\epsilon_a \rho_a d_a g_0 (1 + e)\sqrt{\frac{\Theta_a}{\pi}} + \frac{2\frac{5\sqrt{\pi}}{96}\rho_a d_a \sqrt{\Theta_a}}{(1 + e)\epsilon_a g_0} \times \left[1 + \frac{4}{5} g_0 \epsilon_a (1 + e)\right]^2 \tag{28}$$

where μ_a is the shear viscosity of the solids phase.

The radial distribution function used in the equations above is the equilibrium radial distribution at particle contact derived from statistical mechanics. It can be seen as a measure for the probability of inter-particle contact. The equation of Sinclair[24] is used in this work

$$g_0 = \left[1 - \left(\frac{\epsilon_a}{\epsilon_{a,max}}\right)^{\frac{1}{3}}\right]^{-1} \tag{29}$$

where $\epsilon_{s,max}$ is the maximum solids packing 0.65.

Frictional stress

In the extreme dense regions of the bed ($\epsilon_a \approx \epsilon_{a,max}$), the particle stresses are dominated by interparticle friction rather than by their binary collisions and fluctuating motion. The two-dimensional (2-D) stress tensor for a granular material, which is in the state close to yielding, is proposed by Sokolovski[25] and Jackson[26]:

$$\mu_a = \frac{P_a^* \cdot \sin\phi}{\epsilon_a \sqrt{\frac{1}{6}\left(\left(\frac{\partial u_a}{\partial x} - \frac{\partial v_a}{\partial y}\right)^2 + \left(\frac{\partial v_a}{\partial y}\right)^2 + \left(\frac{\partial u_a}{\partial x}\right)^2\right) + \frac{1}{4}\left(\frac{\partial u_a}{\partial y} + \frac{\partial v_a}{\partial x}\right)^2}} \tag{30}$$

where ϕ is the angle of internal friction, u and v are the velocity components, and x and y are the Cartesian directions of u and v.

Details on the Calculation and Validation Procedure

Experiments

To validate the performance of the cohesive model suggested, and the outcome of the numerical simulations, we have used the experimental data obtained by Ellis and coworkers.[28,29] In those studies, the authors performed a comprehensive experimental study of the hydrodynamics of several gas-solid fluidized-bed reactors, operated with different types of FCC particles. In this work, we have chosen to simulate the hydrodynamics of the unit whose behavior is documented with the most detailed set of data. Table 1 summarizes properties of the bed used for that purpose. The flow field in the unit was investigated by means of optical and capacitance probes. Further details related to experimental data can be found in the work cited.

Numerical simulations

The operating conditions and simulation model parameters used in the computations are summarized in Table 2. The fluidizing gas is, as in the experiments, at ambient temperature and pressure. In this work, we have used the commercial CFD solver FLUENT 6.2, in which the governing equations are solved using the finite volume approach. Since the principal goal here is to investigate the possibility of introducing an agglomeration model into the Eulerian framework, we have decided to perform 2-D simulations as a first step. Provided that the model turns able to reproduce the correct physics of fluidizing cohesive particles, the future work will deal with 3-D simulations.

Table 1. Operating Conditions, Taken From the Experimental Work

Temperature	Ambient
Column diameter (m)	0.29
Height of the unit (m)	4.5
Particle size (μm)	59
Static bed height (m)	0.5
Fluidization velocities (m/s)	0.3; 0.4; 0.5
Minimum fluidization velocity (m/s)	0.0026

Table 2. The Fluidized Bed Operating Conditions and Key Model Parameters Employed in the Simulations

Fluidization velocities (m/s)	0.1; 0.3; 0.5
Particle size (μm)	60
Particle density (kg/m^3)	1530
Bulk density (kg/m^3)	880
Bed width (m)	0.3
Bed height (m)	1.3
Grid size (mm)	4
Time step (s)	$1.0 \cdot 10^{-5}$
Maximum number of iterations per time step ($-$)	30
Convergence criteria for mass	10^{-4}
Coefficient of restitution	0.9
Parameter Φ	1

The discretization of the computational domain and the choice of the time step and convergence criteria (see Table 2) secured the convergence and stability of the numerical procedure. Also, to correctly capture the physics of the processes involved, the time step of the simulations has been selected approximately an order of magnitude larger than the time scale of the cohesive force, and of the collisional time scale. The latter was calculated using the kinetic theory of granular flow formalism; for details of the calculation procedure see Peirano and Leckner.[27] In this work, it was found to be between 6.5×10^{-6} s and 1×10^{-8} s, depending on the fluidization conditions. On the other hand, the time scale for the cohesive force can only be roughly estimated. Here, we have chosen to do this by integrating the equation of motion if only the cohesive force were present. Taking into account the value of the relevant parameters for the cases treated here (e.g., maximal and minimal distances between the particles for which the force is significant, see the following discussion, properties of the particles and the estimation of their velocities), this time scale was always found to be smaller than 5.5×10^{-6} s. Finally, grid independency studies were carried out and we found that grid sizes between 3 and 10 mm show relatively independent and satisfying results. For that purpose, inspection of a behavior of an averaged pressure drop, as a standard procedure in the numerical simulations of fluidized beds, was carried out. To obtain the pressure-velocity coupling, the phase-coupled SIMPLE (PC-SIMPLE) algorithm was used.[30]

The initial gas velocity in the domain corresponds to the minimum fluidization velocity. A uniform gas inlet velocity profile is set at the bottom of the bed. To break the symmetry of the simulations, initially a small off-center jet is introduced for a short period of time. At the wall, there is a no-slip condition for the gas phase. The wall boundary conditions for the particulate phase correspond to an elastic wall-particle collision model (i.e., no dissipation of granular energy at walls of the bed). The boundary condition at the top of the column is a Neumann pressure boundary, with the atmospheric pressure as reference pressure. The flow is assumed fully developed in the free-board above the bed, and to fulfill this condition, the vertical dimension of the domain must be high enough. For the conditions employed here, a column height of 1.3 m is assumed sufficient. Finally, the restitution coefficient used in the simulations was 0.9. It was indicated before that the particles are assumed nearly elastic; this value of the restitution coefficient ensures that

there is a dissipation of energy of fluctuating motion of particles (Eq. 26).

The numerical analysis consists of two parts: first, the comprehensive parametric analysis of the polynomial (Eq. 15) is performed, and second, the model (Eq. 15) is incorporated into the two-fluid simulations. For finding roots of Eq. 15, a hybrid algorithm, consisting of a bisection and Newton-Raphson method, is employed. In the simulations, averaging time of 20 s was assumed sufficient, excluding the initial period of about 5 s needed to reach an overall steady state in the simulations. A number of additional seconds was available for the analysis, but their inclusion in the averaging time had no significant impact on the results.

Parameters of the model

A number of parameters has to be estimated when the analysis of Eq. 15 is to be made. The Hamaker constant A in Eq. 13 is a complex function of several properties of the material, and of the flow situation treated[18]: temperature, dielectric constant of particles, index of refraction of particles and the Planck and Boltzmann constants, among others. The constant is generally assumed to be of the order of magnitude between 10^{-19} and 10^{-23} J. For the solid particles used in the present work, the literature suggests values of approximately 10^{-20}J, but other values were tested in the analysis as well.

The parameter k in Eq. 8 can be readily estimated, provided that the Young modulus of elasticity, E, and the Poisson's ratio v, are known. The parameter δ, representing the typical distance between the particles, is a function of the particle properties and of the flow field. In this work, we have chosen to adopt the value suggested in literature, 3–5 nanometers,[31] for the size of particles and the material used in the simulations. Through the numerical procedure one has to have in mind that Eq. 13 shows a numerical singularity when the distance between two particles approaches zero. In practice, the latter will never occur, since there is a short range repulsion between particles.[31] To prevent this from happening in a numerical framework, a minimum value of that distance is usually introduced. In that sense, the literature suggests the value of 0.5 nm,[31] which is used also in this study. Finally, we will use the granular temperature obtained from the kinetic theory of granular flow to calculate the relative velocity between colliding particles.

Analysis of the agglomeration model

As mentioned previously, finding the roots of a fourth-order polynomial is not a trivial task. There exists a number of classical procedures, which are characterized with varying degrees of speed and certainty toward the answer. Typically, the methods that are certified to converge are often the most slowest, whereas those that are known to reach a solution rapidly, may not converge. A detailed analysis of the most commonly used models, together with some general discussion related to convergence, can be found in, for example, *Numerical Recepies*.[32] In this work, a hybrid algorithm, representing a combination of a bisection (that can never fail to find a root) and a Newton-Raphson's method (the most efficient one) is used. Briefly, the bisection method uses the fact that if a function changes sign within a certain interval, it means that it has to pass through zero. Then the function is evaluated at the interval's midpoint and its sign examined. Whichever limit has the same sign, it is replaced by the midpoint again. As a consequence, each iteration decreases the bounds containing a root by a factor of two. The number of iterations to achieve a solution is, thereby, determined solely by the initial bracketing interval and the desired tolerance in the solution. On the other hand, the Newton-Raphson's method utilizes a Taylor series expansion of a function and practically extends the tangent line at the chosen point until it crosses zero. The newly obtained value at the abscissa determines another point of the function, from which a tangent line is to be extended. The procedure repeats itself until desired convergence criteria are met.

When determining the roots, the most important step is to define the accuracy with which the root finding process is reasonable. The latter implies two things practically: first, when defining a convergence criterion, one has to already have a relatively qualified expectation of the results (i.e., to understand the physics of the process investigated), and second, to have in mind that the solutions obtained are not the exact roots of the polynomial investigated. Very often it is suggested that convergence should be specified by a relative criterion (i.e., in a dimensionless form), but this may cause problems for roots close to zero. Having in mind the expected value of the agglomerate size (to be discussed later), we have assumed convergence to 10^{-9} reasonable.

When solving the polynomial, Eq. 15, the original particle diameter d_p, is taken as a starting point. Multiple roots can be obtained from the equation, and a number of these roots may be unphysical. To bound the agglomerate diameter, this diameter is assumed not to exceed the cell size (4 mm in this work), even if Eq. 15 may have such roots. Taking the cell size as an upper limit for the agglomerate diameter is arbitrary; a fixed number times the particle diameter can be selected as well (such as 65 d_p). Agglomerate diameters lower than the original particle diameter (60 μm) are not tolerable either. A parametric analysis of Eq. 15 readily reveals that, when cohesive forces are relatively small (e.g., for values of the Hamaker constant of the order of 10^{-22}), the balance of forces is reduced to gravity and collisional forces, with drag forces playing a minor role. Under the physical parameters encountered during fluidized-bed operation, and with a low-value for the Hamaker constant, the resulting agglomerate size predicted by our model is very close to the original particle size, as expected. However, when physical parameters outside of this range are considered, unphysical values of the agglomerate size may theoretically occur, due to the unpredictable nature of fourth-order polynomials.

Results

Figure 1 compares the simulated and the experimentally obtained time-averaged solid volume fraction profiles when interparticle forces are not taken into account. As expected and confirmed before by several research groups, e.g.,[9,11] the figure shows a severe over-prediction of the bed height. The model obviously predicts a radically low-particle concentration, and furthermore, with almost no radial variation present. Taking into account the model derived in this work, that pre-

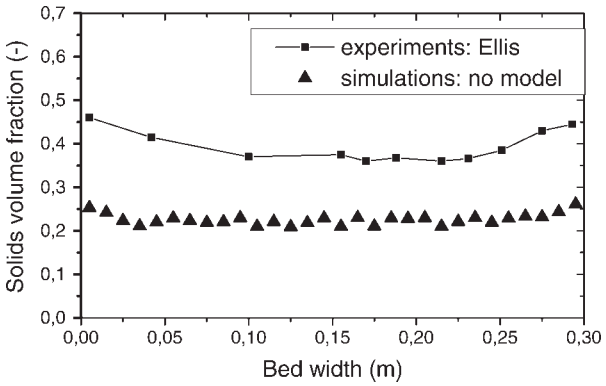

Figure 1. The experimental (■) and simulated (▲) time-averaged solid volume fraction profiles along the bed width, at $h = 0.27$ m height.

The fluidization velocity is $U = 0.3$ m/s. Interparticle forces are neglected in the simulations, leading to an erroneous prediction.

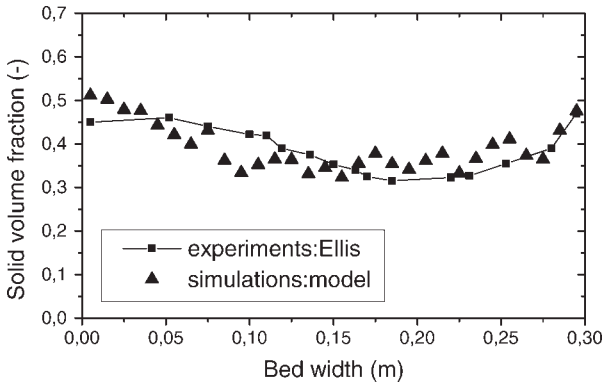

Figure 3. The experimental (+) and simulated (▲) time-averaged solid volume fraction profiles at $h = 0.40$ m height, along the bed width.

The fluidization velocity is $U = 0.3$ m/s. The simulations were done with interparticle forces and the agglomeration model developed in this work.

dicts the formation of agglomerates, the situation is notably changed for the same fluidization conditions, see Figure 2. The general trend of the solids volume fraction is now simulated correctly. In the core region of the bed, the simulations reveal a somewhat lower particle volume fraction, which means that the upward flow of bubbles is slightly miscalculated. On the other hand, possible discrepancies between the simulations, and the experiments in the wall region can originate from the nature of the wall boundary conditions, or from the fact that some effects were not considered in the study (e.g., electrostatic forces between the wall and the solid particles). Figure 3 provides similar trends showing the solids concentration profile at the same fluidization velocity, but recorded somewhat higher in the bed. When the fluidization velocity is considerably increased (from 0.3 to 0.5 m/s), the model still performs effectively, see Figure 4, and with similar general features identified in the lower velocity case. Figure 5 summarizes the previous findings, showing the supremacy of the model (Eq. 15) when expansion of the bed is studied. Figures 6, 7, and 8 illustrate the key effect of the coexistence of hydrodynamic and interparticle forces when fine particles are fluidized. The presence of the cohesive force leads to agglomeration and, as a consequence, the effective particle diameter is increased. The agglomerate diameter presented in Figure 6 corresponds to the fluidization conditions depicted in Figure 2, whereas the diameters in Figures 7 and 8 are related to Figures 3 and 4, respectively. The results for the agglomerate diameter are scaled with the particle diameter. The fact that d_a is several times larger than d_p, as well as some other features of the polynomial (Eq. 15), will be further discussed following.

Discussion

The main objective of this work is to perform Eulerian simulations of the fluid dynamics of dense particulate flows operated with fine powders, without introducing empirical data, artificial parameters or scaling factors to close the cohe-

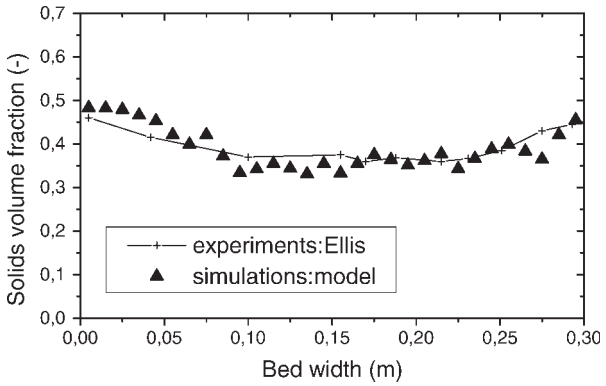

Figure 2. The experimental (+) and simulated (▲) time-averaged solid volume fraction profiles at $h = 0.27$ m height, along the bed width.

The fluidization velocity is $U = 0.3$ m/s. The simulations were done with interparticle forces and the agglomeration model developed in this work.

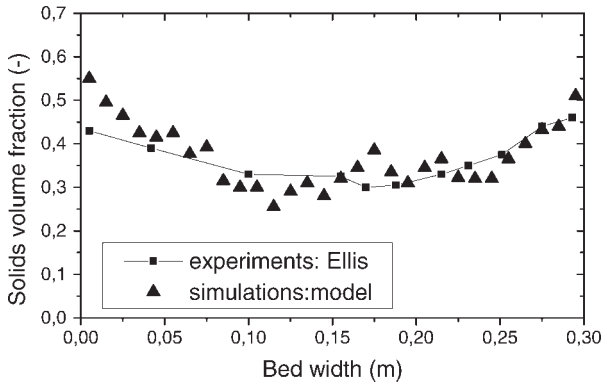

Figure 4. The experimental (■) and simulated (▲) time-averaged solid volume fraction profiles at $h = 0.27$ m height, along the bed width.

The fluidization velocity is $U = 0.5$ m/s. The simulations were done with interparticle forces and the agglomeration model developed in this work.

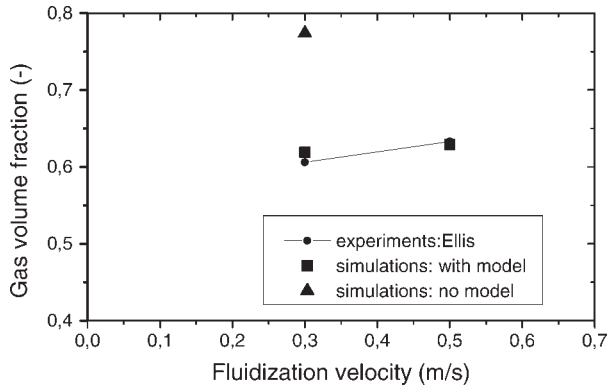

Figure 5. The average solid volume fraction at height $h = 0.27$ m for the experiments (●) compared to two simulation models, the model without agglomeration model (▲), and the model including the agglomeration model (■).

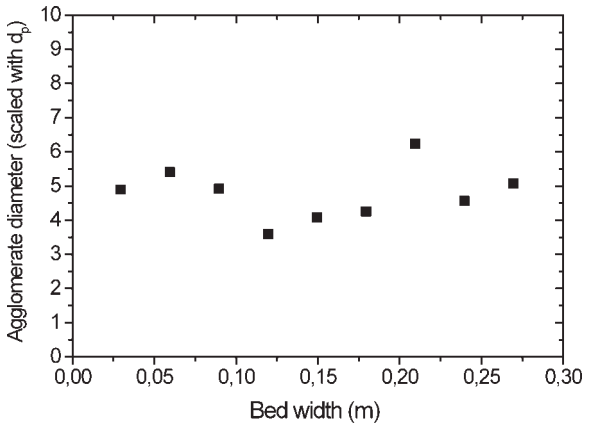

Figure 7. The average size of the agglomerates scaled with the particle diameter at height $h = 0.40$ m, predicted from the agglomeration model for particle size $d_p = 60$ μm.

The fluidization velocity is $U = 0.3$ m/s.

sive model. The goal is to obtain a straightforward model that provides an adequate representation of fluid dynamics of such processes at larger scale (e.g., industrial conditions). The essence of the procedure is to implement realistic representations of forces acting locally on particles in such a suspension.

As Figures 2–5 indicate, introduction of the model, Eq. 15, resulted in the correct overall behavior of the system investigated, which proves that cohesive forces do play an important role in such flows. The bed maintained noncirculating behavior (in reality, in such fluidization conditions a recirculation part of the reactor is needed), although fluidization velocity in all cases significantly exceeds the terminal velocity of a single particle of the original size. A distinctly heterogeneous structure of the bed, with bubbles and gas voids present, was obtained by the simulations. It is interesting to note here that, for units of smaller size and for lower fluidization velocities, Lagrangian simulations have shown that the strong cohesive forces may even preserve the homogeneous fluidization as the intermediate regime between the minimum fluidization velocity U_{mf}, and the minimum bubbling velocity U_{mb}.[33] In units of larger size, however, this regime is difficult to maintain.

A number of important aspects of the model need to be additionally addressed here. The first question ponders the general form of the four forces, whose local balance leads to Eq. 15. There is not much dispute in literature in the way the three of them (gravity, collisional and cohesive forces) are modeled. In contrast, the proper description of the drag force in gas-solid flows has already taken a lot of effort, and it is still far from general agreement in the research community. On the whole, there are two types of approaches when quantifying the drag force in gas-solid flows: models based on macroscopic balances (e.g., using bed pressure drop data or bed expansion experiments) and models obtained from simu-

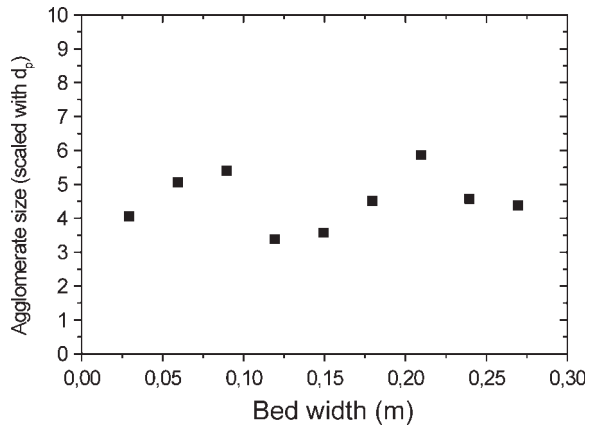

Figure 6. The average size of the agglomerates scaled with the particle diameter at height $h = 0.27$ m, predicted from the agglomeration model for particle size $d_p = 60$ μm.

The fluidization velocity is $U = 0.3$ m/s.

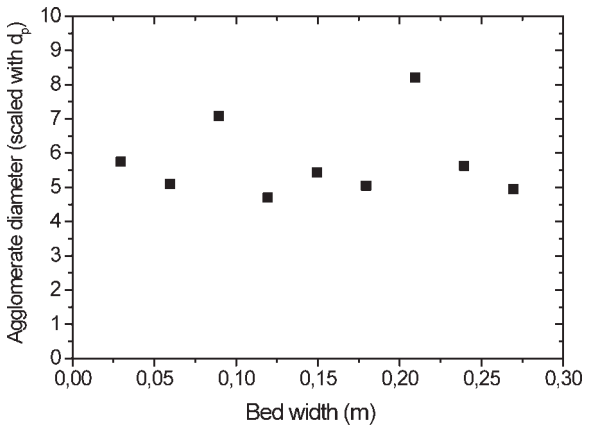

Figure 8. The average size of the agglomerates scaled with the particle diameter at height $h = 0.27$ m, predicted from the agglomeration model for particle size $d_p = 60$ μm.

The fluidization velocity is $U = 0.5$ m/s.

lations on a microscale (e.g., Lattice-Boltzmann methods, see Hill et al.[34] and a discussion on some important issues of their application to gas-solid fluidized beds by Benyahia et al.[35]). The latter models provide detailed information on both the drag force acting on a single particle and on the effect of the adjacent particles. Also, they are reported to be more suitable for capturing the heterogeneous flow structure of the dense gas-solid flows.[36] Yet, in this article we have adopted the traditional and well established Wen and Yu[15] drag force model for the following reasons: the microscale models mentioned earlier are still at an early stage of development and employment, and, furthermore, they result in expressions of relatively high complexity, which are not suitable for introducing in first-order accuracy models as the one proposed in this work. It is then a natural question is then whether a different model than the one we used here would give rise to another form of the agglomerate diameter polynomial, Eq. 15, and, possibly, to a different outcome of the entire procedure. We believe that this will not be the case, since all linear drag models have, in essence, the same type of dependence of the drag force on the particle diameter. As indicated before, the models differ between themselves in the way the presence of other particles is taken into account, whether the random moving of particles is considered etc., all of which would have no effects on the subject of interest in this work. As a final point here, it is to be noted that we did not need to directly modify the drag force model to account for the presence of cohesive powders in the flow field; it is the employment of the agglomerate diameter during the calculation procedure that causes change in the magnitude of the drag force.

Second, it is to be noted here that we have assumed constant the void fraction inside the agglomerate. This, again, may be accepted as a first approximation; there are detailed studies by Keith Watson and co-workers[37] who claim that the void fraction should be a function of the agglomerate diameter for the flow of very fine, cohesive powders. However, we believe that the assumption made does not affect the general conclusions of the procedure proposed. Future work will deal with details of the flow field inside the agglomerate.

Finally, the nature of two parameters still remains the subject of debate. The first one is the Hamaker constant employed in the calculation of the van der Waals forces, which, at present, can be considered approximate. At the moment, there seems to be no alternative to using expressions of the form of Eq. 12, and values for the Hamaker constant found in literature for the same type of particles. The second parameter, the distance between particles δ, incites a similar discussion. Here, we have also adopted values suggested in literature. However, since we believe that promising results have been obtained by the approach proposed, a modeling work on that parameter, which aims at taking into account the heterogeneous distribution of particles within a computational cell, is intended and will be introduced in the future work.

Conclusions

The hydrodynamic behavior of a fluidized bed, operated with FCC particles and at different fluidization velocities, has been investigated by means of computational fluid dynamics (CFD). An approximate model is derived, taking into account the interparticle forces, such as cohesion and collisions, buoyancy, as well as the common hydrodynamic forces, such as drag, to estimate the size of the local agglomerates created in the bed. A comprehensive parametric analysis has illustrated that the proposed agglomerate model is important to determine the effect of cohesiveness of fine particle fluidization. The numerical simulations have shown that an effective particle agglomerate diameter of an order of several times the original FCC particles diameter is obtained. The closure models, describing the hydrodynamics of the particulate phase, are adjusted accordingly. Time-averaged solids volume fraction profiles are in good agreement with experimental data available from literature when the cohesive model is incorporated into the two-fluid approach. The model can be further improved, provided that the more accurate prediction of the van der Waals forces becomes available. Also, further modeling work on the distance between the particles when cohesive forces become important is needed. Finally, future work is planned to introduce the modeling procedure suggested into 3-D simulations and computations of larger units.

Literature Cited

1. Geldart D. Types of gas fluidization. *Powder Technol*. 1973;7:285.
2. Kunii D, Levenspiel O. *Fluidization Engineering*. Second edition Butterworth-Heinemann; 1991.
3. Umekage T, Inaba T, Yuu S. Numerical simulation of air and particles motions in circulating fluidized bed using hard sphere model, DSMC method and LES model, and experimental verification. *Kagaku Kogaku Ronbushu*. 2007;33:6–15.
4. Lun CKK, Savage SB, Jefferey DJ, Chepurniy N. Kinetic theories for granular flow: inelastic particles in Couette flow and slightly inelastic particles in a general flowfield. *J of Fluid Mechanics*. 1984; 140:223–256.
5. Enwald H, Peirano E, Almstedt AE. Eulerian two-phase flow theory applied to fluidization. *Int J Multiphase Flow*. 1996;22:21–66.
6. Wachem BGM, Schouten JC, Krishna R, Bleek CM Van, Sinclair JL. Comparative analysis of CFD models of dense gas-solid systems. *AIChE J*. 2001;46:1035–1051.
7. Ferschneider G, Mege P. Eulerian simulation of dense phase fluidized beds. *Revue de l'I.F.P*. 1996;51.
8. Krishna R, Baten JM. Using CFD for scaling up gas-solid bubbling fluidised bed reactors with Geldart A powders. *Chem Eng J*. 2001; 82:247–257.
9. McKeen T, Pugsley T. Simulation and experimental validation of a freely bubbling bed of FCC catalyst. *Powder Technol*. 2003;129: 139–152.
10. Sharma S, Pugsley T, Delatour R. Three-dimensional CFD model of the deaeration rate of FCC particles. *AIChE J*. 2006;52:2391–2400.
11. Zimmermann S, Taghipour F. CFD modeling of the hydrodynamics and reaction kinetic of FCC fluidized-bed reactors. *Indian Eng and Chem Res*. 2005;44:9818–9827.
12. Kim H, Arastoopour H. Extension of kinetic theory to cohesive particle flow. *Powder Technol*. 2002;122:pp 83–94.
13. Gidaspow D, Huilin L. Equation of state and radial distribution functions of FCC particles in a CFB. *AIChE J*. 1998;44:279–293.
14. Ye M, Hoef MA, Kuipers JAM. From discrete particle model to a continuous model of Geldart A particles. *Chem Eng Res and Des*. 2005;83:833–843.
15. Wen CY, Yu YH. Mechanics of fluidization. *Chem Engg Progr Symposium Series*. 1966;62:100–111.
16. Walton OR. Computer Simulation of Rapidly Granular Solids Tech. Rep. UCRL-99545 Lawrence Livermore National Laboratory; 1988.
17. Timoshenko SP, Goodier JN. *Theory of Elasticity*. McGraw-Hill, New York; 1970.
18. Israelachvili J. *Intermolecular and surface forces: with applications to colloidal and biological systems*. Academic Press, London; 1985.

19. Zhou T, Li H. Estimation of agglomerate size for cohesive particles during fluidization. *Powder Technol*. 1999;101:57–62.
20. Wachem BGM, Schaaf J, Schouten JC, Krishna R, Bleek CM Van. Experimental validation of Lagrangian-Eulerian simulation of fluidized beds. *Powder Technol*. 2001;116:155–165.
21. Ding J, Gidaspow D. A bubbling fluidization model using theory of granular flow. *AIChE J*. 1990;36:523–538.
22. Jenkins JT, Savage SB. A theory for the rapid flow of identical, smooth, nearly elastic, spherical particles. *J of Fluid Mech*. 1983;130: 187–202.
23. Gidaspow, Bezburuah R, Ding J. Hydrodynamics of Circulating Fluidized Beds; Kinetic Theory Approach Fluidization VII, Proceedings of the 7th Engineering Foundation Conference on Fluidization. 1992:75–82.
24. Sinclair JL, Jackson R. Gas-particle flow in a vertical pipe with particle-particle interactions. *AIChE J*. 1989;35:1473.
25. Sokolovski VV. *Statistics of Granular Media*. Pergamon Press; 1965.
26. Jackson R. Some mathematical and physical aspects of continuum models for the motion of granular materials. In: *Theory of Dispersed Multiphase Flow*. Meyer RE, ed. Academic Press; 1983;291–338.
27. Peirano E, Leckner B. Fundamentals of turbulent gas-solid flows applied to circulating fluidized bed combustion. *Progr in Energy and Comb Sci*. 1998;24:259–296.
28. Ellis N. Hydrodynamics of gas-solid turbulent fluidized beds. University of British Columbia, Canada; 2003, PhD Thesis.
29. Ellis N, Bi HT, Lim CJ, Grace JR. Hydrodynamics of turbulent fluidized bed of different diameters. *Powder Technol*. 2004;141:124–138.
30. Vasquez SA, Ivanov VA. A phase coupled method for solving multiphase problems on unstructured meshes in ASME 2000 Fluids Engineering Division Summer Meeting; 2000.
31. Shchukin ED. *Colloid and surface chemistry*. Elsevier, Amsterdam; 2001.
32. Press WH, Teukolsky SA, Vetterling WT, Flannery BP. *Numerical Recipies in C*. Cambridge University Press; 1992.
33. Ye M, Hoef MA, Kuipers JAM. A numerical study of fluidization behaviour of Geldart A particles using a discrete particle model. *Powder Technol*. 2004;139:129–139.
34. Hill RJ, Koch DL, Ladd Anthony AJC. The first effects of fluid inertia on flows in ordered and random arrays of spheres. *J of Fluid Mech*. 2001;448:213–241.
35. Benyhia S, Syamlal M, O'Brien TJ. Extension of Hill-Koch-Ladd dragg correlation over all ranges of Reynolds number and solids volume fraction. *Powder Technol*. 2006;162:166–174.
36. Li J, Kuipers JAM. Gas-particle interactions in dense gas-fluidized beds. *Chem Eng Sci*. 2003;58:711–718.
37. Watson P Keith, Valverde JM, Castellanos A. The tensile strength and free volume of cohesive powders compressed by gas flow. *Powder Technol*. 2001;115:45–50.

Manuscript received Dec. 22, 2006, and revision received Aug. 27, 2007.